Modeling the Nitrogenase FeMo Cofactor

Thomas H. Rod and Jens K. Nørskov*

Contribution from the Center for Atomic-scale Materials Physics (CAMP), Department of Physics, Building 307, Technical University of Denmark, DK-2800 Lyngby, Denmark

Received April 3, 2000. Revised Manuscript Received August 25, 2000

Abstract: Density functional calculations are used to describe the nitrogenase FeMo cofactor and its interaction with N_2, H_2, H_2O, and CO. Different models of the active part of the cofactor are investigated, and it is shown that a detailed description of the adsorption of different substrates can be obtained in good agreement with available experimental information. In addition, we propose a reaction path for the catalytic synthesis of ammonia through the gradual hydrogenation of molecular N_2 adsorbed on the Fe part of the cofactor.

1. Introduction

Nitrogen fixation−the conversion of atmospheric nitrogen into biologically accessible forms−is a difficult process due to the extraordinary strength of the dinitrogen bond. Despite the abundance of atmospheric nitrogen, the access to nitrogen is often the limiting factor for plant growth. There are three main sources of biologically accessible nitrogen, (i) oxidation of N_2 to nitrogen oxides by lightning and combustion, (ii) the industrial Haber−Bosch process where N_2 reacts with hydrogen over an Fe- or Ru-based catalyst to form ammonia, and (iii) the enzyme-catalyzed ammonia synthesis where N_2 reacts with electrons and protons to form ammonia. Ammonia is the product in the latter two reactions, which may be summarized by the schemes:

$$\begin{aligned} &\text{Haber−Bosch:} && N_2 + 3H_2 \rightarrow 2NH_3 \\ &\text{Nitrogenase:} && N_2 + 8H^+ + 8e^- \rightarrow 2NH_3 + H_2 \end{aligned} \quad (1)$$

Apart from the catalysts, the main difference between the two ammonia synthesis processes is that the Haber−Bosch process uses gaseous hydrogen (H_2), and needs high temperatures and pressures, about 400 °C and 100 atm,[1] while the enzyme process uses solvated hydrogen ($H^+ + e^-$) and at least 16 adenosine triphosphate (ATP) for each N_2 fixated.[2,3] The enzyme functions under ambient conditions (room temperature and 1 bar).

Much effort has been invested in resolving the mechanisms of the two ammonia synthesis catalytic processes, and the combination of experimental and theoretical work has resulted in a detailed picture of the reaction path for the Haber−Bosch process.[4] A similarly detailed mechanism for the enzyme reaction is still not available, mainly because it has not been possible to directly detect the interaction of N_2 with the enzyme.

In the present paper, we suggest a possible reaction mechanism for the enzyme process. Our suggestion is based on an extensive set of density functional calculations of the interaction between N_2 and a simple model of the active site of the enzyme. We also investigate the transfer of electrons and protons to the active site and the gradual hydrogenation of the nitrogen. In addition we study the adsorption of CO at the active site. CO is known to be an inhibitor for ammonia synthesis and we explain why. CO has also been used as a probe of the active site, since its adsorption properties can be probed spectroscopically. We show that our model describes these properties quite well, lending additional credibility to the model and the computational approach employed. Finally, we discuss the H_2 production and the HD reaction on the active site.

The paper is organized as follows. We first briefly review the experimental knowledge that has been assembled about the structure and overall function of the enzyme. Previous theoretical work is also discussed. We then go on to discuss the computational method we use and the clusters we use to model the FeMoco. The main results are organized under five headings: H bonding and H_2 formation, CO adsorption, hydrogenation of adsorbed N_2, and proton transfer to adsorbed N_2 and CO. Finally, we discuss the results in the light of available experimental observations, and show that we have a molecular level picture of the process which can explain a number of observations regarding the properties of the FeMoco and the catalytic ammonia synthesis.

2. Previous Work

2.1. Structure and Properties of the Enzyme. A large amount of knowledge has been assembled about the enzyme. It consists of two metalloproteins termed the Fe protein and the MoFe protein after their constituent metal clusters. The Fe protein contains a ferredoxin (4Fe-4S), and the MoFe protein contains two pairs of unique clusters, namely the P-cluster and the FeMo cofactor (FeMoco).[5] The latter is most likely the active site where N_2 binds and is reduced.[3]

During each enzyme turnover the two protein components form a complex, which presumably is the transition state for the over-all enzyme reaction. During the lifetime of that complex one electron is transferred from the ferredoxin in the Fe protein to the FeMoco and the substrate in the MoFe protein, along with hydrolysis of ATP.

The crystal structures of the protein components are known from X-ray diffraction for a number of bacteria,[6−8] and are in

* Address correspondence to this author. E-mail: norskov@fysik.dtu.dk.

(1) Tennison, S. R. In *Catalytic Ammonia Synthesis Fundamentals and Practice*; Jennings, J. R., Ed.; Plenum Press: New York, 1991; p 303.

(2) Stryer, L. *Biochemistry*, 4th ed.; W. H. Freeman and Company: New York, 1995; p 714.

(3) Burgess, B. K.; Lowe, D. J. *Chem. Rev.* **1996**, *96*, 2983−3012.

(4) *Frontiers in catalysis: ammonia synthesis and beyond*, Vol. 1 of *Topics in Catalysis*; Topsøe, H., Boudart, M., Nørskov, J. K., Eds.; Baltzer: Basel, 1994.

(5) Howard, J. B.; Rees, D. C. *Chem. Rev.* **1996**, *96*, 2965−2982.

10.1021/ja001163q CCC: $19.00
Published on Web 12/06/2000

reasonable agreement with extended X-ray adsorption fine structure studies (EXAFS).[9−11]

The structure of an ADP·AlF_4 stabilized complex resembling the transition state has been resolved as well.[12]

As previously mentioned, the FeMoco is most likely the active site, where N_2 binds and is reduced. The FeMoco has the stoichiometric formula $MoFe_7S_9$ and is bound to the protein through the end Fe atom and through Mo. The Fe is coordinated by a cysteine residue, and Mo is coordinated by a histidine residue (Figure 1). Mo is in addition coordinated by a carboxylate and the hydroxy group of homocitrate (cf. Figure 1). The structure of the FeMoco can be considered as a metal core with sulfur evenly distributed on it. Six of the Fe atoms in the core form a prism and are only 3-fold coordinated. The three central sulfur atoms (μ_2S) bridge two iron atoms each, while the remaining six sulfurs (μ_3S) bridge three iron atoms each.

Mo can be substituted by V or Fe without destroying the ability of the enzyme to make ammonia.[13] With the possible exception of *Rhodobacter capsulatus*, the enzyme activity is however reduced such that the sequence of activities is as follows: Mo > V > Fe.[13] On the basis of the different activities, the difference in activation energies can, however, be estimated to be of the order of 5 kJ/mol.

Electron spin resonance (ESR) spectroscopy shows that in the so-called resting state or semireduced state of the FeMoco the total spin is $S = {}^3/_2$, which changes to integer nondetectable states if the FeMoco is either oxidized or reduced.[14] Besides changing the spin, X-ray crystallography of both the semireduced and oxidized FeMoco[7,8] and EXAFS[5,11] shows that there are no major structural changes associated with changes of the redox levels of the FeMoco, apart from a small contraction of the Fe−Fe bond lengths which is observed for the reduced state of the FeMoco.

The FeMoco may be isolated from the protein into a solution of *N*-methylformamide (NMF). This was first done by Shah and Brill in 1977.[15] EXAFS and ESR studies demonstrate that the cofactor is extracted intact from the MoFe protein.[10] In fact, the extracted cofactor can be added to cofactor-deficient MoFe proteins, in which case the enzyme restores its activity. It has also been demonstrated that the reactivity of the isolated FeMoco is much the same as in the enzyme, since it can form H_2[16] (see later), adsorb CO[17] (see later), and protonate acetylene.[18]

The above studies indicate that the structure of the FeMoco is quite robust. We will exploit this below, when formulating a model of the FeMoco that can be handled computationally.

Many kinetic data exist that describe the reactivity of nitrogenase. These are reviewed by Burgess[19] and Burgess and Lowe.[3] The reactivity of the isolated FeMoco was most recently reviewed by Smith et al.[20]

Here we will focus on the reactivity of nitrogenase toward dinitrogen, hydrogen, and carbonmonoxide, which are the molecules we have studied in connection with the FeMoco.

2.1.a. Dinitrogen. N_2 is reduced according to the scheme

$$N_2 + 6H^+ + 6e^- \rightarrow 2NH_3 \qquad (2)$$

along with H_2 evolution. So far it has not been possible to directly detect the interaction of N_2 with the FeMoco, which strongly indicates that the N_2 bonding state is weakly bound or metastable.

The stoichiometry of H_2 formation is still unknown. The ratio between consumed N_2 and produced H_2 increases with increasing electron flow. It is further found that H_2 inhibits ammonia synthesis.[3,19,21]

One of the intermediates in the hydrogenation of N_2 to NH_3 has been shown to be hydrazine (N_2H_4).[19] It is therefore not surprising that hydrazine also can be hydrogenated by nitrogenase by the scheme:

$$N_2H_4 + 2H^+ + 2e^- \rightarrow 2NH_3 \qquad (3)$$

On the basis of available kinetic data, Thorneley and Lowe[21] have developed a model for the ammonia synthesis with the assumption that N_2 replaces H_2, i.e., with a minimum stoichiometry of N_2:$H_2 = 1$. In the scheme N_2 is irreversibly activated after three to four enzyme turnovers, and N_2 is directly hydrogenated with hydrazine as one of the intermediates. In the Thorneley−Lowe scheme H_2 can on the other hand evolve after two, three, and four enzyme turnovers.

CO inhibits the hydrogenation of N_2 and of hydrazine, with the result that the entire electron flux goes to the formation of H_2.

2.1.b. Hydrogen. In the absence of N_2 and other reduceable molecules, the electron flow goes entirely to the reduction of protons, according to the scheme

$$2H^+(aq) + 2e^- \rightarrow H_2 \qquad (4)$$

H_2 can also be adsorbed as demonstrated by the HD formation during enzyme turnover in an atmosphere of D_2 and N_2. It is not known if N_2 is a prerequisite for HD formation, but N_2 significantly enhances the tendency for D_2 dissociation on the complex.[3,19,21] At a more detailed level, stopped-flow experi-

(6) Georgiadis, M. M.; Komiya, H.; Woo, D.; Kornuc, J. J.; Rees, D. C. *Science* **1992**, *257*, 1653−1659. Kim, J.; Rees, D. C. *Nature* **1992**, *360*, 553−560. Kim, J.; Rees, D. C. *Science* **1992**, *257*, 1677−1682. Chan, M. K.; Kim, J.; Rees, D. C. *Science* **1993**, *260*, 792−794. Bolin, J. T.; Ronco, A. E.; Morgan, T. V.; Mortenson, L. E.; Xuong, N. *Proc. Natl. Acad. Sci. U.S.A.* **1993**, *90*, 1078−1082. Kim, J.; Woo, D.; Rees, D. C. *Biochemistry* **1993**, *32*, 7104−7115.

(7) Peters, J. W.; Stowell, M. H. B.; Soltis, M.; Finnegan, M. G.; Johnson, M. K.; Ress, D. C. *Biochemistry* **1997**, *36*, 1181−1187.

(8) Mayer, S. M.; Lawson, D. M.; Gormal, C. A.; Mark Roe, S.; Smith, B. E. *J. Mol. Biol.* **1999**, *292*, 871−891.

(9) Chen, J.; Christiansen, J.; Tittsworth, R. C.; Hales, B. J.; George, S. J.; Coucouvanis, D.; Cramer, S. P. *J. Am. Chem. Soc.* **1993**, *115*, 5509−5515. Chen, J.; Christiansen, J.; Campobasso, N.; T., Bolin J.; Tittsworth, B. C.; Hales, B. J.; Rehr, J. J.; Cramer, S. P. *Angew. Chem., Int. Ed. Engl.* **1993**, *32*, 1592−1594. Eady, R. R.; Smith, B. E.; Abraham, Z. H. L.; Dodd, F. E.; Grossman, J. G.; Murphy, L. M.; Strange, R. W.; Hasnain, S. S. *J. Phys. IV* **1997**, *7*, 611−614.

(10) Liu, H. I.; Filipponi, A.; Gavini, N.; Burgess, B. K.; Hedman, B.; Cicco, A. D.; Natoli, C. R.; Hodgson, K. O. *J. Am. Chem. Soc.* **1994**, *116*, 2418−2423. Harvey, I.; Strange, R. W.; Schneider, R.; Gormal, C. A.; Garner, C. D.; Hasnain, S. S.; Richards, R. L.; Smith, B. E. *Inorg. Chim. Acta* **1998**, *275*−276, 150−158.

(11) Christiansen, J.; Tittsworth, R. C.; Hales, B. J.; Cramer, S. P *J. Am. Chem. Soc.* **1995**, *117*, 10017−10024.

(12) Schindelin, N.; Kisker, C.; Schlessman, J. L.; Howard, J. B.; Rees, D. C. *Nature* **1997**, *387*, 370−376.

(13) Eady, R. R. *Chem. Rev.* **1996**, *96*, 3013−3030.

(14) Rees, D. C.; Chan, M. K.; Kim, J. *Adv. Inorg. Chem.* **1993**, *40*, 89−119.

(15) Shah, V. K.; Brill, W. J. *Proc. Natl. Acad. Sci. U.S.A.* **1977**, *74*, 3249−3253.

(16) Le Gall, T.; Ibrahim, S. K.; Gormal, C. A.; Smith, B. E.; Pickett, C. J. *Chem. Commun.* **1999**, (9), 773−774.

(17) Ibrahim, S. K.; Vincent, K.; Gormal, C. A.; Smith, B. E.; Best, S. P.; Pickett, C. J. *Chem. Commun.* **1999**, (11), 1019−1020.

(18) Bazhenova, T. A.; Bazhenova, M. A.; Petrova, G. N.; Shilova, A. K.; Shilov, A. E. *Russ. Chem. Bull.* **1998**, *47*, 861−867.

(19) Burgess, B. K. In *Molybdenum Enzymes*; Spiro, T. G., Ed.; Wiley-Interscience: New York, 1985; Chapter 5, pp 161−219.

(20) Smith, B. E.; Durrant, M. C.; Fairhurst, S. A.; Gormal, C. A.; Grönberg, K. L. C.; Henderson, R. A.; Ibrahim, S. K.; Gall, T. Le; Pickett, C. J. *Coor. Chem. Rev.* **1999**, *185*−186, 669−687.

(21) Thorneley, R. N. F.; Lowe, D. J. In *Molybdenum Enzymes*; Spiro, T. G., Ed.; Wiley-Interscience: New York, 1985; Chapter 5, pp 221−285.

ments demonstrate that only one enzyme turnover (one electron and proton) is needed to produce HD. Experiments using tritium, T_2, show that less than 2.4% of the formed HT ends in the solvent as T^+. These observations result in the following reaction scheme for the formation of HD:

$$2H^+(aq) + 2e^- + D_2 \rightarrow 2HD \qquad (5)$$

Most recently Le Gall et al.[16] demonstrated that H_2 formation could be electrocatalyzed by the isolated FeMoco in a NMF solvent, provided that the chemical potential of the reacting electrons was increased relative to H_2. This demonstrates that the FeMoco can be active when isolated from the enzyme.

2.1.c. Carbon Monoxide. As previously mentioned, CO inhibits nitrogen fixation, but not H_2 evolution. CO is generally an excellent probe molecule due to its ability to form stable bonds to metals. This is also the case for CO bonding to the FeMoco, where detailed insight into the dynamics of CO adsorption has been obtained by utilizing the fact that the FeMoco is a spin-polarized cluster, and that the CO stretch frequency is separable from other frequencies in the enzyme.

The ESR spectra have been monitored as CO is adsorbed.[22−25] It has also been possible to detect the hyperfine coupling between the spin-polarized Fe atoms and a spin-active nucleus, suce as ^{13}C, ^{57}Fe, or ^1H (the latter in a D_2O environment), for CO-inhibited FeMoco.[22,23,24]

Two different ESR signals appear for low (0.05−0.08 atm) and high (0.5 atm) pressure. They are interpreted as the binding of one and two CO molecules, respectively.[23,24] The first CO molecule binds strongly, while the second binds weakly even at low temperatures. Hoffman et al.[23] suggest that the first CO molecule bridges two Fe atoms, while adsorption of a second results in both CO molecules to bond on-top to each Fe. It is moreover demonstrated that a hydrogen bond between the protein surrounding and the waist of the FeMoco is lost upon binding of CO.[22]

The above interpretations are supported by measurements of time-resolved infrared spectra of the enzyme during turnover by George et al.[26] One CO-dependent band at 1906 cm^{-1} is observed at lower CO pressure (the gas-phase CO frequency is 2170 cm^{-1}), and if the CO pressure is increased, two new bands appear at higher frequencies (1958 and 1936 cm^{-1}) while the first band disappears.

Ibrahim et al.[17] have shown that the isolated FeMoco can also bind CO, and that the vibrational spectrum of the adsorbed CO is very similar to the corresponding one for the enzyme.

Cameron and Hales[25] have observed that at least one enzyme turnover is needed prior to adsorption of the first CO. This behavior has been confirmed by Ibrahim et al. for the isolated FeMoco.[17] They demonstrated that CO does not bind to the FeMoco before the cofactor is reduced by at least one electron. They have also monitored the time-resolved IR spectra for CO bonding to isolated FeMoco, and find CO frequencies in the same range as George et al.[26] for the cofactor embedded in the enzyme.

2.2. Theoretical Studies. Since the structure of the FeMoco was first reported, several theoretical studies of the electronic properties and the binding of N_2 to a number of iron−sulfur complexes modeling the FeMoco have been published.[27−38] The theoretical studies are generally characterized by making compromises between the accuracy of the electronic structure method and the size of the system included in the modeling of the cofactor.

Deng and Hoffmann[27] used the semiempirical Extended Hückel (EH) approach to study different N_2 bonding modes to a fairly complete model of the FeMoco. Plass[28] compared the electronic structures of the FeMoco and corresponding structures with Mo substituted by V or Fe, also on the EH basis. Plass also studied the activation of N_2 bonding in an end-on fashion to one of the Fe_4 facets of the cofactors. Zhong and Liu[32] have studied the activation of N_2 for different binding modes to the cofactor[33] applying the complete neglect of differential overlap (CNDO) method. In addition, they have studied the energy along different paths for adsorption of N_2.

Stavrev and Zerner have also considered the activation of N_2 for different binding modes to the cofactor[33] applying a combination of the Hartree−Fock (HF) and the semiempirical Intermediate Neglect of Differential Overlap (INDO) method. Applying the same approaches they have also studied different oxidation levels of the FeMoco,[34] and the hydrogenation of an adsorbed N_2 on the FeMoco.[35] Some of the steps in the hydrogenation process have further been studied by more accurate electronic structure methods based on Hartree−Fock theory, Möller−Plesset perturbation theory (MP2), and density functional theory (DFT), with the BLYP and the B3LYP exchange-correlation functional.

DFT calculations have been published by a number of other authors.[29−31,36−38] Dance was the first to use DFT calculations to study N_2 bonding to the FeMoco.[29] His studies are based on a symmetric Fe_8S_9 cluster resembling the metal−sulfur core of the FeMoco, but with Fe substituting Mo and with additional ligating thiol groups. He has used the Local Density Approximation (LDA) or the gradient-corrected BLYP exchange-correlation functional. In these studies the focus has been on N_2 binding to one of the Fe_4 facets of the FeMoco. In addition, Dance has studied a particular mechanism for hydrogenation of N_2 and formation of H_2.[31] It should be noted that the most stable site for N_2 bonding found by Dance is one where N_2 binds on-top to a single Fe atom.[31]

Siegbahn et al.[38] have studied the possibility for N_2 binding in the cavity enclosed by the six 3-fold coordinated Fe atoms by studying the possibility for N_2 to bind in a side-on fashion and bridging two Fe atoms of various iron−sulfide clusters with 2−4 Fe atoms. They have also studied the binding of N_2 to a symmetric Fe_8S_9 cluster. Hydrogenation of N_2 was considered

(22) Lee, H. I.; Hales, B. J.; Hoffman, B. M. *J. Am. Chem. Soc.* **1997**, *119*, 11395−11400.
(23) Lee, H.-I.; Cameron, L. M.; Hales, B. J.; Hoffman, B. M. *J. Am. Chem. Soc.* **1997**, *119*, 10121−10126.
(24) Pollock, R. C.; Lee, H.-I.; Cameron, L. M.; DeRose, V. J.; Hales, B. J.; Orme-Johnson, W. H.; Hoffman, B. M. *J. Am. Chem. Soc.* **1995**, *117*, 8686−8687.
(25) Cameron, L. M.; Hales, B. J. *Biochemistry* **1998**, *37*, 9449−9456.
(26) George, S. J.; Ashby, G. A.; Wharton, C. W.; Thorneley, R. N. F. *J. Am. Chem. Soc.* **1997**, *119*, 6450−6451.
(27) Deng, H.; Hoffmann, R. *Angew. Chem., Int. Ed. Engl.* **1993**, *32*, 1062−1065.
(28) Plass, W. *J. Mol. Struct. (THEOCHEM)* **1994**, *315*, 53−62.
(29) Dance, I. G. *Aust. J. Chem.* **1994**, *47*, 979−990.
(30) Dance, I. *Chem. Commun.* **1997**, (2), 165−166.
(31) Dance, I. *Chem. Commun.* **1998**, (5), 523−530.
(32) Zhong, S.-J.; Liu, C.-W. *Polyhedron* **1997**, *16*, 653−661.
(33) Stavrev, K. K.; Zerner, M. C. *Chem. Eur. J.* **1996**, *2*, 83−87.
(34) Stavrev, K. K.; Zerner, M. C. *Theor. Chem. Acc.* **1997**, *96*, 141−145.
(35) Stavrev, K. K.; Zerner, M. C. *Int. J. Quantum Chem.* **1998**, *70*, 1159−1168.
(36) Rod, T. H.; Hammer, B.; Nørskov, J. K. *Phys. Rev. Lett.* **1999**, *82*, 4054−4057.
(37) Rod, T. H.; Logadottir, A.; Nørskov, J. K. *J. Chem. Phys.* **2000**, *112*, 5343−5347.
(38) Siegbahn, P. E. M.; Westerberg, J.; Svensson, M.; Crabtree, R. H. *Phys. Chem. B* **1998**, *102*, 1615−1623.

for N_2 binding to an Fe dimer, similar to the one employed by Stavrev and Zerner[35] in their DFT calculations. The calculations were based on the most accurate B3LYP exchange-correlation functional.

Rod et al. have studied the reactivity of the FeMoco by using a plane-wave basis set, and with the spin-polarized PW91 exchange-correlation functional.[36] This study was based on a structure consisting of periodically repeated units, each with the stoichiometric formula $MoFe_6S_9$. It was shown that N_2 can bind on-top on one of the Fe atoms and that a mechanism where adsorbed N_2 is hydrogenated stepwise to form two ammonia molecules is possible at low temperature, provided that the chemical potential of the reacting "H" ($=H^+ + e^-$) is higher than that of H_2. Calculations for the same model compared with corresponding calculations for a Ru(0001) surface and calculations for the Haber−Bosch mechanism on Ru(0001) have been used to illustrate why two different mechanism are in use, and the widely different reaction conditions that are required for the enzyme and the metal surface.[37] These latter calculations used the more accurate RPBE functional[39] for the description of the exchange-correlation energy.

Despite the different approaches there are a number of points of agreement between the various calculated results. First, both Dance[31] and Rod et al.[36] find the on-top bonding of N_2 to a single Fe atom to be the most stable. They further agree that the N_2 is loosely bound, but it still distorts the complex such that the Fe atom ends up being trigonally pyramidally coordinated. The on-top bonding mode is also seen for the N_2 binding to a three-coordinated Fe atom of some of the complexes studied by Siegbahn et al. The hydrogenation path found by Rod et al.[37] also agrees with the one found by Stavrev and Zerner.[35]

Finally, the energetics obtained by Siegbahn et al. for N_2 side-on bonding is very similar to that obtained by Rod et al. for N_2 end-on bonding, demonstrating that the obtained energetics is quite general for hydrogenation of N_2.

3. Calculational Details

There are two sets of approximations that are needed to describe the function of an enzyme like nitrogenase theoretically. First, there is the choice of method for solving the electronic structure problem. Second, we have to concentrate on a small part of the protein to make the problem computationally tractable. We include enough of the real protein in our model of the active site that we can assume that it is realistic, but cannot include too much to give a reasonably accurate description of the electronic structure. In the following we look at each of these approximations separately.

3.1. Density Functional Calculations. All our calculations are based on density functional theory, with a plane wave expansion of the Kohn−Sham wave functions and the generalized gradient approximation (GGA) for the exchange-correlation term. The plane wave expansion means that we have to treat a system that is periodic in all three dimensions. For a finite cluster, we accomplish this by repeating a *supercell* containing the cluster periodically in three dimensions including enough vacuum around each cluster to make sure there is no interaction between cells.

Ultra-soft pseudopotentials have been used to describe the core part of the ions,[40] except for sulfur where a soft pseudopotential has been used.[41] Plane waves with kinetic energies up to 25 Ry are included for both the models. Structures and energies for model I (see below) are, unless otherwise stated, calculated self-consistently using the spin-dependent Perdew−Wang (PW91) functional.[42] The calculated densities for spin-up and spin-down electrons are then used as input for a non-self-consistent calculation using the spin-dependent revised Perdew−Burke−Enzerhoff (RPBE) functional, which recently has been shown to describe chemisorption more accurately than PW91.[39] The RPBE functional has, for instance, been able to describe the adsorption and reaction of N_2 on Fe and Ru surfaces semiquantitatively.[43,44] There is therefore good reason to believe that this level of calculation should be sufficient to describe the interaction of N_2 with the FeMoco in some detail. Test calculations show that non-self-consistently calculated RPBE energies only differ by a few J/mol from corresponding self-consistently calculated energies. Structures and energies for model II are calculated self-consistently using the RPBE functional.

The Brillouin zone is sampled by two $\boldsymbol{k}$-points along the c^* axis for model I, while Γ point sampling is used for model II. Fermi population of the Kohn−Sham orbitals with $k_BT = 10$ and 1 kJ/mol for models I and II, respectively, and Pulay mixing of the resulting density have been used.[45] It has been tested that the calculations are converged with respect to the basis set and the number of $\boldsymbol{k}$-points. Sums of atomic densities or a previously calculated wave function have been used as an initial guess for all calculations. Antiferromagnetic and ferromagnetic states have been obtained by starting with a nonzero spin density on each metal atom.

3.2. The Model of the Active Site. As mentioned previously, the FeMoco is believed to be the catalytically active site where N_2 is adsorbed and hydrogenated. We therefore concentrate on this cluster. Both the structure and the interaction of the FeMoco with a substrate like CO appear from several experiments to be quite independent of the detailed surroundings. The CO adsorption and the vibrational spectrum of adsorbed CO are for instance similar whether the FeMoco is in the protein or extracted and solvated. This suggests that it is reasonable, as a starting point only, to consider the FeMoco and its immediate surroundings.

We have employed two models of the FeMoco. The models are shown in Figure 1 together with the ligated FeMoco from the X-ray structure.[46] Model I, to the left in Figure 1, has been constructed from the experimental FeMoco structure by removing the ligands and the terminal Fe atom and then extending the remaining part periodically. This means that the coordination number of the Mo atom is the same in the model as in the real structure, and that the six central Fe atoms are in exactly the same configuration as in the real FeMoco. The resulting infinitely long chains are periodically repeated in the plane perpendicular to the chains, such that we obtain a hexagonal super cell with side lengths $a = 9.5$ Å and $c = 7.75$ Å. The value of c has been chosen to be the value that minimizes the total energy with respect to c, see later. All degrees of freedom have been allowed to relax to the minimum energy structure.

Model II to the right in Figure 1 is made by taking the crystal structure[46] and truncating the ligands Cys, His, and Homocitrate

(39) Hammer, B.; Hansen, L. B.; Nørskov, J. K. *Phys. Rev. B* **1999**, *59*, 7413−7421.
(40) Vanderbilt, D. *Phys. Rev. B* **1990**, *41*, 7892−7895.
(41) Troullier, N.; Martins, José Luís *Phys. Rev. B* **1991**, *43*, 1993−2006.
(42) Perdew, J. P.; Chevary, J. A.; Vosko, S. H.; Jackson, K. A.; Pederson, M. R.; Singh, D. J.; Fiolhais, C. *Phys. Rev. B* **1992**, *46*, 6671−6687.
(43) Mortensen, J. J.; Hansen, L. B.; Hammer, B.; Nørskov, J. K. *J. Catal.* **1999**, *182*, 479−488.
(44) Dahl, S.; Logadottir, A.; Egeberg, R. C.; Larsen, J. H.; Chorkendorff, I.; Törnqvist, E.; Nørskov, J. K. *Phys. Rev. Lett.* **1999**, *83*, 1814−1817.
(45) Kresse, G.; Furthmüller, J. *Comput. Mater. Sci.* **1996**, *6*, 15−16.
(46) PDB ID: 3MIN. Published in ref 7. General PDB refs 60−62.

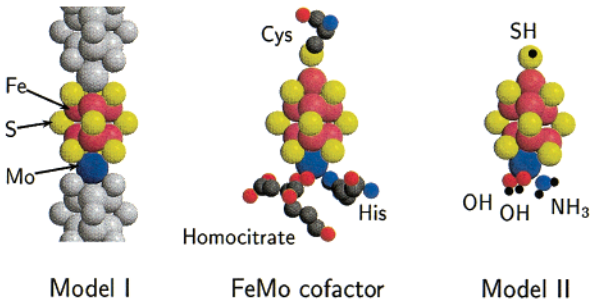

Figure 1. The nitrogenase FeMoco with ligands and the model systems I and II employed in the present study. The shown structures are the calculated energy minima for the model systems, while the structure for the FeMoco is obtained from ref 46. One supercell of model I is colored, and the periodicity along the *c*-axis is shown by the repeated noncolored units. There is a vacuum between the repeated units along the two *a*-axes of I. Only one supercell for II is shown, since there is a vacuum between repeating units along all three supercell axes.

after the first ligating atom. Each of the truncated bonds to the ligating atoms have then been saturated by bonds to H atoms. This means that we have substituted Cys by SH, His by NH_3, and Homocitrate by two OH groups (cf. Figure 1). A preliminary relaxation of the ligands has been made on separate models where only the coordinated metal and the ligands themselves are maintained and where the missing metal−S bonds have been substituted by metal−H bonds. Using the resulting structures, the ligands are then kept fixed in all subsequent calculations, while all the remaining atoms are allowed to relax. The compound is periodically repeated in all directions with a resulting triclinic supercell with axes $a = b = 11$ Å and $c =$ 15.4 Å and angles $\alpha = 90°$, $\beta = 69°$, and $\gamma = 120°$.

The images of the structures in Figure 1, as well as Figures 2−5, 7, 8, and 10−13, have been made by using MolScript 2.1[47] and Raster 3D 2.5.

4. Properties of the Two Model Clusters

The completely relaxed structures of both models are shown in Figure 1. The structural parameters are compared to the experimentally determined bond lengths in Table 1. The agreement is very satisfactory. The results show that the models we consider are stable and that they are reasonable representations of the local properties of the FeMoco.

The electronic structure of the FeMoco is complicated due to antiferromagnetic couplings[48] which result in a low total spin of $S = {}^3/_2$ for the so-called resting state of the enzyme.[3]

We have made spin co-linear calculations for a number of different spin states of the two model clusters. The details will be discussed elsewhere.[49] Here it suffices to discuss the properties of the lowest energy state of the two model systems.

According to our calculations the ground-state spin of model I is $S = 0$, while it is $S = {}^3/_2$ for model II. The low total spin of model I is a consequence of a strong antiferromagnetic coupling. In fact all our results for this model can be described in an Ising model with nearly the same antiferromagnetic coupling describing all the Fe−Fe pairs.[49] The extra 3 spin-up electrons of model II are due to the extra Fe atom in combination with the antiferromagnetic coupling.

Table 1. Bond Lengths for the Relaxed Structure of Models I and II As Shown in Figure 1[a]

	bond lengths (Å)			
bond	*K. pneumoniae*	*A. vinelandii*	DFT (I)	DFT (II)
Mo−μ_3S	2.31−2.38	2.16−2.34	2.48−2.52	2.40−2.48
end Fe−μ_3S	2.21−2.32	2.15−2.31		2.24−2.27
Fe−μ_3S in the Mo end	2.17−2.31	2.10−2.23	2.15−2.18	2.19−2.25
Fe−μ_3S in the Fe end	2.22−2.32	2.11−2.28		2.20−2.30
Fe−μ_2S in the Mo end	2.17−2.25	2.06−2.20	2.10−2.13	2.11−2.16
Fe−μ_2S in the Fe end	2.20−2.24	2.10−2.24		2.13−2.23
Fe−Fe in the Mo end	2.63−2.70	2.45−2.61	2.46−2.54	2.57−2.76
Fe−Fe in the Fe end	2.66−2.72	2.55−2.66		2.59−2.93
Mo−Fe	2.67−2.72	2.60−2.72	2.93−3.04	2.66−2.81
central Fe−Fe	2.59−2.63	2.48−2.60	2.56−2.58	2.58−2.65
end Fe−Fe	2.63−2.67	2.54−2.72		2.58−2.64

[a] The bond lengths are compared with those obtained from the crystal structures from the bacteria *Azotobacter vinelandii*[46] and *Klebsiella pneumoniae*.[63]

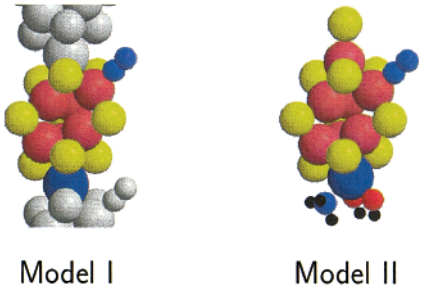

Figure 2. N_2 adsorption on models I and II. The N_2 adsorption energy for model I is 0 kJ/mol and that for II is −10 kJ/mol. The energy for adsorption of N_2 on Fe atoms in the Mo end is expected to be lower due to steric effects. The structures are rotated 180° relative to Figure 1, and N atoms are illustrated with light blue balls.

While there is no reason the small model I should agree in detail with experiment, model II should be directly comparable. In the present case model II has the same total spin as the "resting state", and we therefore tentatively suggest that the model II state represents the resting state of the FeMoco.

Finally, we compare the interaction of the two model clusters with an N_2 and a CO molecule. We consider here adsorption on-top of one of the Fe atoms, since we will show later that this is the most stable adsorption site for both molecules. The structure of the two models with adsorbed N_2 is very similar (cf. Figure 2). In both cases the N_2 distorts the cluster significantly, and the distortion is identical for the two models. The adsorption energy is also quite similar. We find that N_2 binds slightly weaker (by 10 kJ/mol) on model I than on model II. The same behavior is observed for CO adsorption, but in this case CO binds with 100 kJ/mol on model I and 110 kJ/mol on model II. The total spin of model II decreases by one to $S = {}^1/_2$ upon adsorption of both N_2 and CO, which agrees with the experimentally observed spin for CO binding FeMoco.[25] The total spin of model I also changes. For both models the change in the spin is localized to the Fe atom where N_2 or CO binds.

(47) Kraulis, P. J. *J. Appl. Crystallogr.* **1991**, *24*, 946−950.

(48) Münck, E.; Rhodes, H.; Orme-Johnson, W. H.; Davis, L. C.; Brill, W. J.; Shah V. K. *Biochim. Biophys. Acta* **1975**, *400*, 32−53. Huynh, B. H.; Henzl, M. T.; Christner, J. A.; Zimmerman, R.; Orme-Johnson, W. H.; Münck, E. *Biochim. Biophys. Acta* **1980**, *623*, 124−138. Venters, R. A.; Nelson, M. J.; McLean, P. A.; True, A. E.; Levy, M. A.; Hoffman, B. M.; Orme-Johnson, W. H. *J. Am. Chem. Soc.* **1986**, *108*, 3488−3498. True, A. E.; Nelson, M. J.; Venters, R. A.; Orme-Johnson, W. H.; Hoffman, B. M. *J. Am. Chem. Soc* **1988**, *110*, 1935−1943.

(49) Rod, T. H. Density Functional Calculations and Modeling of the Biological Ammonia Synthesis. Ph.D. Thesis, Center for Atomic-scale Materials Physics (CAMP), Department of Physics, Technical University of Denmark, 2000. Rod, T. H.; Nørskov, J. K. To be submitted for publication.

We conclude on this basis that the local chemistry of the two model compounds is quite similar, and in the following we will concentrate on the smaller, computationally simpler model I.

Here and in the following the adsorption energy is defined as the total energy of the structure, X (e.g. model I), with the adsorbate, A (e.g. N_2), adsorbed minus the sum of the total energies of the bare structure X and the adsorbate A isolated from each other, i.e.

$$E_{ads} = E_{tot}(X - A) - (E_{tot}(X) + E_{tot}(A)) \qquad (6)$$

Model I is best suited to study the chemistry associated with the six central Fe atoms, since their nearest and next nearest neighbors are identical to those (in the Mo end) of the real FeMoco. The Mo atom, on the other hand, has sufficiently different surroundings that its chemistry may be different. We therefore concentrate in the present study on reactions associated with the central Fe atoms. This does not exclude that reactions associated with the Mo atoms can be important in connection with the FeMoco, but as we have mentioned Mo can be replaced by V or Fe in the enzyme without loss of the ability to produce ammonia, suggesting that Mo may not be the active site. The present work also demonstrates that many experimental observations can be explained by chemistry associated with the Fe atoms.

5. H Bonding and H_2 Formation

Before discussing the interaction of the model FeMoco with substrates such as CO or N_2, we first study the effect of an electron and proton flow to the FeMoco. As a starting point, we have added 1−4 H atoms ("H" = e^- + H^+) to model I. The configurations we study in this way correspond to configurations after an equal number of electrons and protons have been transferred to the cluster.

The H atoms have been added to the μ_3S atoms (coordinated to three metal atoms), to the μ_2S atoms (coordinated to two metal atoms), and to the Fe atoms, and combinations thereof. The results are summarized in Figure 3. It is seen that a single H atom binds most strongly to a μ_2S atom (Figure 3a), and less so to an Fe atom (Figure 3c), and binds weakest to a μ_3S atom (Figure 3b). Zero-point energies are not included in the energy diagram in Figure 3, but the difference in zero-point energy for an H atom bonded to an Fe atom and an H atom bonded to an S atom has been calculated to be too small to change the relative stability of the structures in Figure 3.

The H atoms continue to be most stable at the μ_2S atoms as more H atoms are added. The first three H atoms therefore prefer to bind to the three μ_2S atoms. The fourth one added prefers to bind to an Fe atom (Figure 3k). The latter state is meta-stable compared to the state in Figure 3l where H_2 is formed on one of the Fe atoms, and this state is again meta-stable compared to H_2 far away from the complex and the structure in Figure 3d. A continuous flow of electrons and protons to the complex therefore results in H_2 formation by the scheme in Figure 3 provided saturation of the complex with hydrogen is achieved. For a sufficiently high chemical potential of the electrons and protons this process may be nonactivated.

For sufficiently low H_2 pressure and electron-transfer rate, H_2 may evolve after addition of only two H atoms (Figure 3, d → f → g) or three H atoms (Figure 3, h → i → j) in agreement with the Thorneley−Lowe scheme. If the H atoms relax on the μ_2S atoms (where they are most stable) before forming H_2 this process is activated, since it costs energy to form the intermediate hydrides.

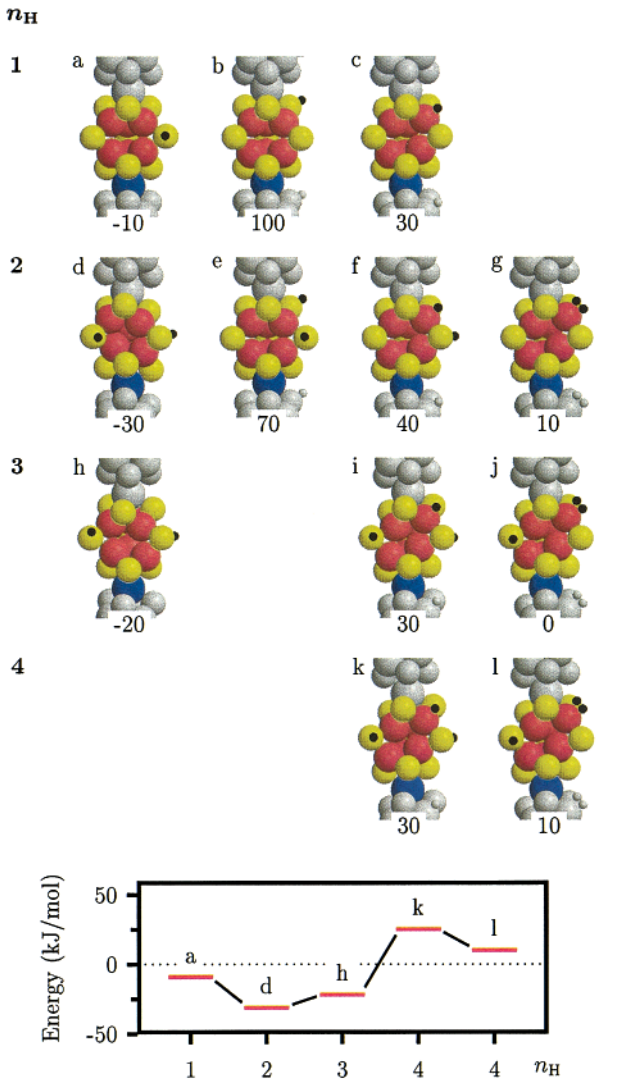

Figure 3. H binding structures of I. The same number n_H of H atoms (shown by black balls) are bound to structures in the same row, and the number is given to the left of each row. The accumulated adsorption energies relative to the hydrogen free I and the gas-phase molecule H_2 are given (in kJ/mol) immediately below each structure. The energy of the most stable structure as hydrogen is added one by one is shown in the lower panel.

Table 2. Adsorption Energies for H_2 Side-On Adsorption, N_2, and CO On-Top Adsorption, and H_2O and NH_3 Adsorption on an Fe Atom of Model I for 0−3 H Atoms Bonded to the Central μ_2S Atoms[a]

n_H	H_2	N_2	CO	H_2O	NH_3
0	10	0	−100	20	−90
1	10	0	−100		
2	40	20	−80		
3		−10			

[a] All energies are in kJ/mol.

The reverse process, H_2 adsorption, is only slightly activated (Table 2). H_2 adsorption becomes more stable as the number of H already on the complex decreases, and dissociation to μ_2S atoms is possible if they are not already occupied.

6. CO Adsorption

CO is the substrate of FeMoco that has been best characterized spectroscopically in the adsorbed state. Comparing the

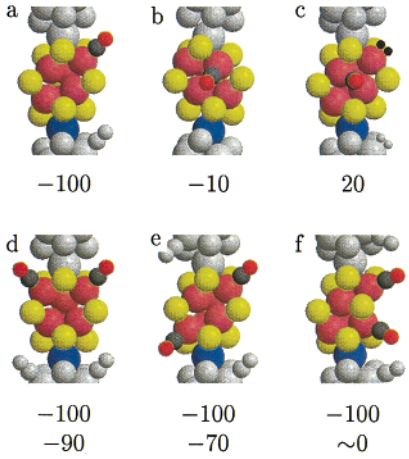

Figure 4. CO adsorption on the model system I. CO has been added ontop (a, b) and bridge (c). Two CO molecules may be adsorbed as well (d−f). The adsorption energies are given (in kJ/mol) below each structure. In the case of the structures in parts d−f, the adsorption energy of both the first CO molecule (upper value) and the second CO molecule (lower value) is given. The structure in part f has not been completely relaxed, because of its relatively high energy. C atoms are illustrated with gray balls and O atoms with red balls.

calculated and the experimental results is a good test of our ability to describe the adsorption properties of the FeMoco theoretically, and we therefore discuss CO adsorption on our model FeMoco in some detail before continuing with our treatment of the adsorption and hydrogenation of N_2.

As discussed above, it is known from experiment that (1) CO is an inhibitor for N_2 adsorption,[19] (2) at least one electron (and proton) transfer is needed prior to CO adsorption,[17,25] (3) the FeMoco is capable of binding two CO molecules,[23,24,25,26] and the binding of the second CO is reversible,[25] (4) the CO stretch frequency decreases significantly due to adsorption on the FeMoco,[17,26] and (5) an H-bond to the "waist" of the cofactor is broken upon CO adsorption.[22]

We have tried to let CO adsorb in a number of different sites on model I. In each case we then relax the system to the closest low-energy configuration. It can be seen in Figure 4 that the most stable adsorption geometry by far is one where the CO molecule binds end-on with the C atoms on-top of a single Fe atom. The bond energy is about 100 kJ/mol.

By adsorbing H atoms on the cluster, we can change the formal oxidation state of the cluster, but that hardly changes the adsorption strength (Table 2). The spin density on the Fe to which the CO bonds decreases significantly.

To test the possibility of double CO occupancy on model I, we have added another CO molecule after the first one. The other CO molecule has been added on top of each of the three chemically distinct Fe atoms (Figure 4d−f). It can be seen that the complex is able to bind a second CO, and the adsorption energy is slightly smaller than for the first CO (Figure 4d,e).

We have calculated the shifts in the CO stretch frequencies due to adsorption in the most stable structures.[50] The shifts are listed in Table 3 together with the experimentally observed shifts at low and high CO coverage. CO adsorption on the FeMoco lowers the stretch frequency according to our calculations, and it can be seen that if there are two adsorbed CO molecules they both have frequencies close to the one observed for a single CO. This is qualitatively in agreement with the experimental observations,[17,26] but the frequency shifts we find are too small.

(50) The reason why we report the shifts, rather than the absolute frequencies, is that we find the shifts to be nearly independent of the way we sample the CO stretch potential curve, as long as the samplings are equal. This is true even if we sample in the nonharmonic part of the potential.

Table 3. Shifts in CO Stretch Frequencies Due to Adsorption on I[a]

structure	$\Delta\omega_1$ (cm^{-1})	$\Delta\omega_2$ (cm^{-1})
Figure 4a	−126	
Figure 4d	−126	−136
experiments		
1 CO	−264	
2 CO	−212	−234

[a] Both shifts are given for structures which bind two CO molecules. The experimental values are for CO adsorbing to the FeMoco embedded in the enzyme.[26]

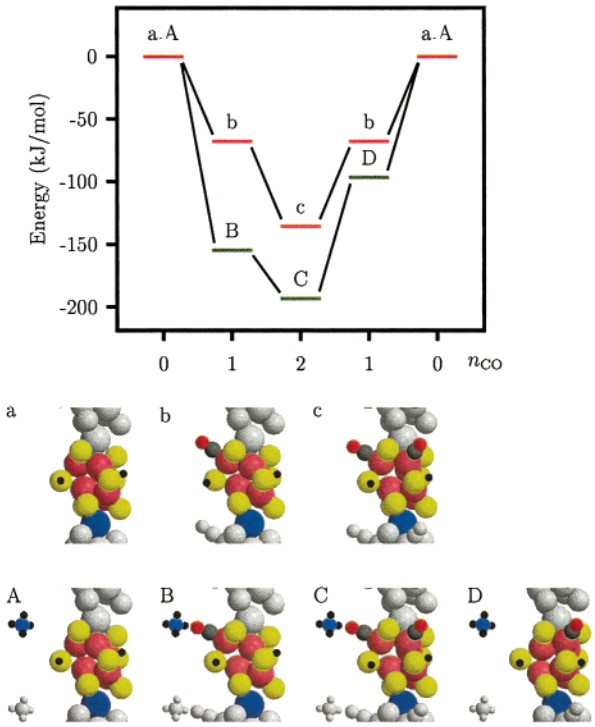

Figure 5. Single and double CO adsorption with and without a proton donor for adsorption of a single CO close to the proton donor site (B), for adsorption of a second CO away from the proton donor site (C), and finally for adsorption of a single CO on an Fe away from the proton donor (D). The results are compared with corresponding ones, calculated by exactly the same setup, but without the proton donor NH_4, Figure 5a−c. The upper panel shows the accumulated adsorption energy for each structure.

Reducing the oxidation state of the cluster by adding hydrogen atoms to the central μ_2S atoms and/or adding H_2 to an Fe as in Figure 4c does not change the frequencies appreciably.

We can also reduce the oxidation state of the cluster by transferring an electron without a simultaneous transfer of a proton. We have modeled this situation in the following way. It is clear that the enzyme must have sites close to the active site that can act as proton donors during nitrogen hydrogenation. Such a donor might either be an amino residue or an H_2O molecule, of which there are several in the proximity of the cofactor. We therefore add to our system a weak base, NH_3 (or H_2O later) in the vicinity of the cofactor (see Figure 5A). We can then add an electron and a proton to the base. It turns out, as expected, that the electron ends up on the cluster, and we therefore have a model where the cluster has been reduced and the negative ion is "screened" by a surrounding "solvated" proton. This is a very primitive model, which only serves to illustrate the possible role of independent electron and proton

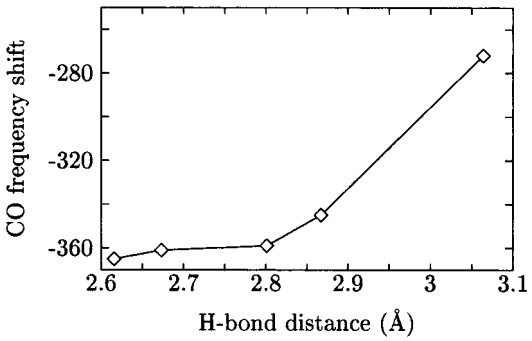

Figure 6. The CO stretch frequency shift for CO adsorbed on I and H-bonded to NH_4^+ as function of the H-bond distance.

transfer and the possible role of the proton donor in stabilizing intermediates on the cofactor. We will show below that such a model can account for a number of the observed properties of CO on the cofactor.

In these calculations one of the *a* axes has been expanded to 13 Å, to make room for the NH_4^+ ion. All calculations are made for structures where two of the μ_2S atoms each bind an H atom. In light of the previous discussion (Section 5) three H atoms would have been more natural, but the actual number of H atoms is generally unimportant for the results. The N of NH_4^+ (or O of H_3O^+) and the Mo atom have been constrained in space during these calculations.

The energetics for CO adsorption employing this setup is shown in Figure 5. The results are striking. The electron transfer and the inclusion of the proton donor in the form of NH_4^+ significantly increases the energy gain due to adsorption of the first CO (Figure 5B), while the energy gain (E(B) − E(C)) due to adsorption of a second CO molecule is decreased.

An interesting question is whether the observed effects are caused by the electron transfer or by the interaction with the nearby proton donor. To answer this question we have calculated the energy of CO in the structure in Figure 5D. In that case the CO is pointing away from the proton donor, and therefore there is no H-bonding to the donor. The cluster still has an extra electron, though. By comparing the adsorption energies for Figure 5D and Figure 5b it can be seen that the change of the adsorption energy is smaller but still significant. We therefore conclude that the electron transfer is only a part of the change in adsorption energy in the structure in Figure 5B. The polarization of the cluster−CO bond due to the proton provides an additional effect.

The electron transfer and the vicinity of the proton donor also affects the CO vibrational frequencies. When the proton donor is close, the shift becomes even larger than observed experimentally, but the frequency shift depends critically on the distance between the proton donor and the CO molecule (Figure 6). A frequency shift of the right magnitude is clearly possible for reasonable values of the CO−proton distance. A look at the frequency shift for CO pointing away from the proton donor shows that the charge transfer alone is enough to change the vibrational frequency sizably (Table 4).

We are now in a position to compare our calculated results to the experimental observations 1−5 discussed above: (1) CO is clearly an inhibitor for N_2 adsorption since CO adsorbs much stronger than N_2 (see below). (2) The transfer of an electron to the cofactor and a proton to the vicinity of the cofactor greatly enhances the stability of adsorbed CO. (3) The FeMoco can bind two CO molecules and the first CO binds stronger than the second one. (4) The CO stretch frequency decreases significantly due to adsorption on the FeMoco. The second CO has a smaller frequency shift than the first. (5) If the proton donor was placed in the same distance to the O atom but more below the CO like the His-195 in the *Azotobacter vinelandii* MoFe protein, the H^+ might have been able to form a hydrogen bond to the closest μ_2S atom. The H bonding to CO may therefore very well be the exchangeable H observed in the absence of CO.

We conclude that the calculations give a quite reasonable description of the experimental observations.

Based on the reports by Newton et al.[51] we suggest that histidine-195 of *Azotobacter vinelandii* (histidine-194 of *Klebsiella pneumoniae*) may be the group H-bonding to a first adsorbed CO. Later on we discuss this further.

Table 4. The Frequency Shifts for CO Bonded End-On to Fe and H-Bonded to NH_4^+

structure[a]	$\Delta\omega$ cm^{-1}
b (no H-bond)	−136
B (d = 2.67 Å)	−361
D (d = ∞)	−197
B′ (d = 3.06 Å)	−272

[a] The letters in the column refer to the labels in Figure 5. The d values in parentheses are the H-bond distances.

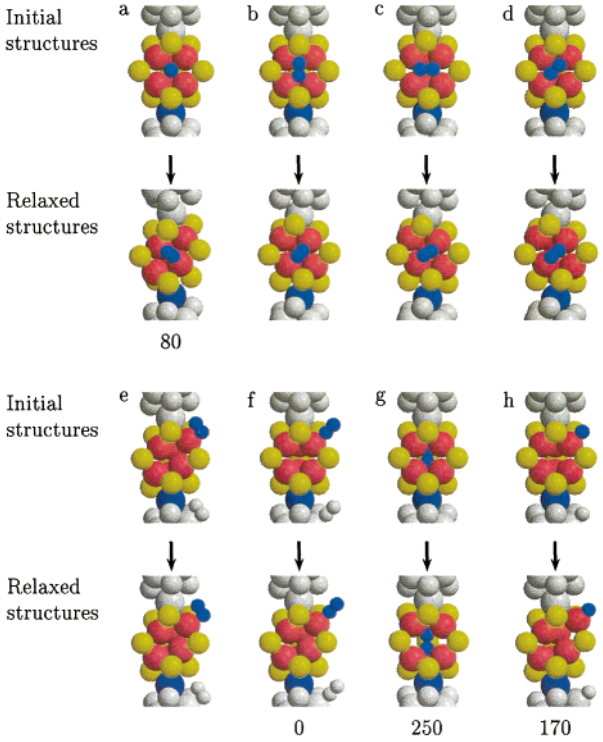

Figure 7. Different structures tried for N_2 adsorption. All the initial structures are shown. The arrows indicate the end structures due to relaxation. Calculated N_2 adsorption energies (in kJ/mol) are given below each of the relaxed structures.

6.1. N_2 Adsorption. To explore where molecular N_2 binds to our model (I) FeMoco, we have added N_2 in a number of different ways to the cluster and then relaxed all the ionic degrees of freedom. In Figure 7 we show both the initial and final relaxed structures as well as the adsorption energy relative to molecular N_2. Positive values of the adsorption energy mean that the molecule is most stable in the gas phase far from the cluster.

(51) Kim, C.-H.; Newton, W. E.; Dean, D. R. *Biochemistry* **1995**, *34*, 2798−2808. Dilworth, M. J.; Fisher, K.; Kim, C.-H.; Newton, W. E. *Biochemistry* **1998**, *37*, 17495−17505.

In the case where N_2 is added standing up in the Fe_4 hollow site (Figure 7a), the N_2 ends up bonded on-top a single Fe. In all cases where N_2 is added side-on to the Fe_4 facet (Figure 7b−d), the relaxation of the complex results in N_2 bonded in a similar, tilted on-top position. The N_2 side-on addition to a single Fe atom (Figure 7e) also results in an upright on-top adsorption geometry.

Finally, we have tested the possibility of N_2 binding in the Fe_6 cavity (Figure 7g) and the possibility for dissociation of N_2 by calculating the binding energy for a single N atom (Figure 7h).

The most stable structure is the one shown in Figure 7f, where N_2 binds linearly on-top of an Fe atom. The relative stability of the configurations in Figure 7 does not change if the complex is stretched. We have also tried to stretch the structure with N_2 in the Fe_6 cavity (Figure 7g) with two H atoms bonded to the central μ_2S atoms. The structure continues, however, to be highly unstable.

Based on the considerable energy separation between the on-top structure in Figure 7f and the other structures and the insensitivity of these energy differences on the geometry and the number of H atoms on the cluster, we suggest that the structure in Figure 7f is the most interesting for further study.

Relaxation of the complex is essential for N_2 adsorption. The energy gain by relaxing the structure is as high as 160 kJ/mol. The relaxation results in a distortion of the complex, such that the Fe atom that binds N_2 is pulled away from the three enclosing S atoms (Figure 7f). We suggest that this is mainly due to a direct repulsive interaction between the N_2 molecule and the S atoms. We note that this is a very general phenomenon. The same type of distortion is found when CO or H_2 is adsorbed and for the larger model II (cf. Figure 2). Such repulsive interactions between adsorbates and preadsorbed S have also been observed at metal surfaces.[52]

We have calculated the N_2 adsorption energy for complexes with H atoms bonded to the central μ_2S atoms to study how N_2 adsorption is affected by the reduction level of I. We generally find the adsorption energy to be only slightly dependent on the number of H atoms on the cluster (cf. Table 2).

The bond strength for H_2O is smaller than that for N_2 (cf. Table 2), and water is therefore only a weak inhibitor for nitrogen fixation. This is clearly important for a reaction taking place in an aqueous medium.

We note that the simple on-top N_2 adsorption site is well-known from surfaces[43,53,54] and other N_2 bonding complexes.[55] Note also that H_2 can adsorb on the same site as N_2, and therefore H_2 is expected to inhibit nitrogen fixation, at least for high H_2 pressures.

The adsorption of N_2 on the neutral, isolated cluster is essentially thermoneutral according to our calculations. Even in cases where the N_2 is meta-stable it does not desorb in our calculations. The reason is that there is a barrier for adsorption/desorption. This is, however, quite different if we transfer the electron to the cluster and the proton to the proton donor, as modeled in our calculations by the setup in Figure 8A (the same as Figure 5A). This changes the stability of the adsorbed N_2 molecule significantly. The effect is completely analogous to the one we have observed for CO adsorption. The conclusion from this is that activation of N_2 is much more likely during turnover, where electrons are transferred to the FeMoco and protons to its vicinity. In the next section we will then discuss the further proton transfer to the N_2 molecule.

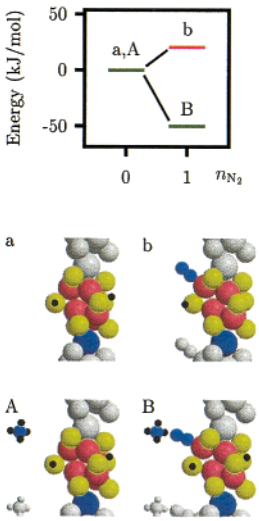

Figure 8. N_2 adsorption on I with and without a proton donor in the vicinity of N_2. The second H atom on the structure in part b is, as an exception, placed on the third μ_2S atom. The adsorption of N_2 without a proton donor is here slightly endothermic, since two H atoms are bound to the μ_2S atoms (see also Table 2).

7. Hydrogenation of Adsorbed N_2

We now turn to the question of the ammonia synthesis reaction. We note first that atomic N is extremely unstable on the cluster (cf. Figure 7h). We therefore exclude the possibility that N_2 dissociates before hydrogenation. This is very different from the situation on a metal surface, where the dissociated state is much more stable than the molecularly adsorbed state and where dissociation is a prerequisite for ammonia synthesis.[4,43,54]

The only possibility for forming ammonia is then if the adsorbed N_2 is directly hydrogenated. In the following we first study the simultaneous addition of electrons and protons to N_2 adsorbed on model cluster I. In the subsequent section we then consider the proton-transfer process.

The calculated energies for all possible intermediates during hydrogen addition to the cluster with and without adsorbed N_2 are shown in Figure 9.

From Figure 9 we can find the reaction path for N_2 hydrogenation for the case where all hydrogens are mobile. The path is found by picking out the most stable intermediate with a given number of hydrogens. The structures of the most stable intermediates are shown in Figure 10.

The first three H atoms transferred to the complex prefer to bind to each of the central μ_2S atoms. Because the N_2 adsorption is almost thermoneutral, N_2 can adsorb and desorb several times as the first three H atoms are added. The fourth hydrogen prefers to bind directly to the adsorbed N_2 (Figure 10f). This state is meta-stable compared to adsorbed hydrazine. The S bound H atoms can therefore migrate from the S atoms to the N_2 (Figure 10f−i). Addition of a fifth hydrogen to the Fe bound N splits off ammonia (Figure 10j), and yet another hydrogen forms adsorbed ammonia, which eventually desorbs.

We note, that even though the last ammonia desorption step is uphill in energy, desorption will be easy if the ammonia pressure is low. We also have not included solvent effects which will increase the tendency for ammonia desorption. Addition

(52) Mortensen, J. J.; Hammer, B.; Nørskov, J. K. *Surf. Sci.* **1998**, *414*, 315−329.
(53) Mortensen, J. J.; Morikawa, Y.; Hammer, B.; Nørskov, J. K. *J. Catal.* **1997**, *169*, 85−92.
(54) Bozso, F.; Ertl, G.; Grunze, M.; Weiss, M. *J. Catal.* **1977**, *49*, 18−41.
(55) Leigh, G. J. *Acc. Chem. Res.* **1992**, *25*, 177−181.

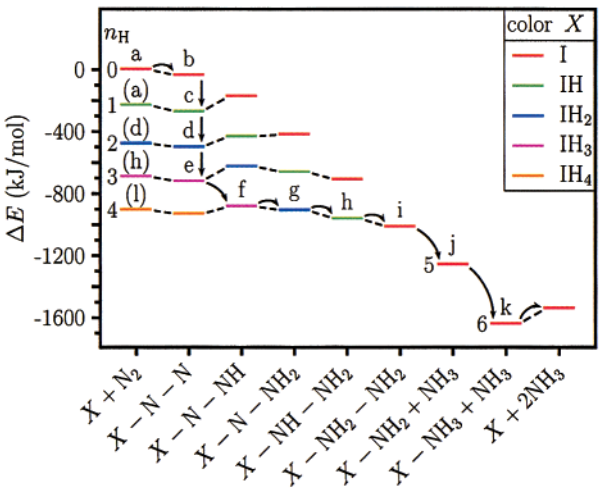

Figure 9. The calculated binding energy ΔE of N_2 and H to model I. The binding energies are relative to N_2(g), H atoms, and model I. Along the horizontal axis it is shown whether N_2 is adsorbed and how many H atoms are bound to the adsorbed N_2. Going down from one structure to the next in the vertical direction corresponds to the addition of hydrogen to the body of the complex. Energy bars for systems with the same total number of H atoms, n_H (on the N_2 and on the body of the complex), are connected by dashed lines, and n_H is shown to the left of the left-most bar. The arrows connect the most stable intermediates as N_2 is adsorbed and H atoms are added one by one. The labels a−k refer to the corresponding structures in Figure 10 and the labels in parentheses refer to the structures in Figure 3. All the energies in the present diagram are calculated by using the PW91 functional, which results in a small decrease (by ∼40 kJ/mol) of the N_2 adsorption energy relative to RPBE calculated energies.

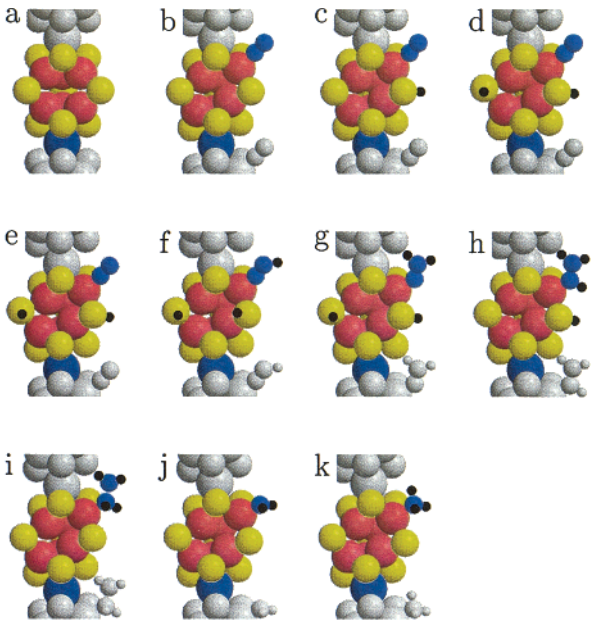

Figure 10. Calculated structures of the lowest energy configuration of model I (a), with N_2 adsorbed (b), with 1−3 H atoms (c−e), 4 H atoms (f−i), and 5,6 H atoms (j, k). In case of the structures in parts e and f, the unseen H atom is bound to the hidden μ_2S atom. In each case several different configurations have been considered, but it cannot be excluded that configurations may exist that are not found by the used energy minimization routine. The scenario presented is therefore a possible one, but not necessarily the only one.

of a seventh hydrogen to the adsorbed ammonia results in the immediate desorption of an ammonium ion, leaving a negatively charged complex model I behind.

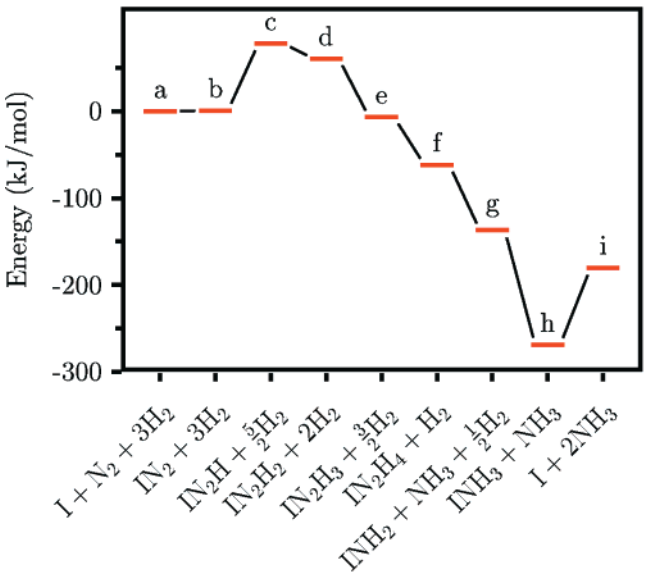

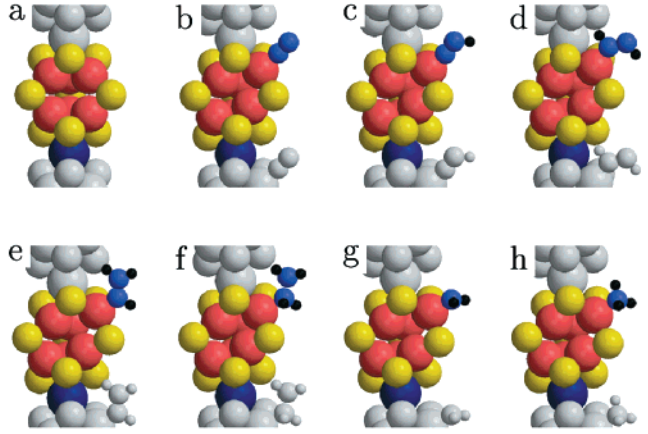

Figure 11. Energy diagram for the hydrogenation of N_2 on model I. In the top panel the calculated binding energies of the intermediates along the reaction path for hydrogenation of N_2 on model I are plotted. The binding energies are relative to the gas-phase molecules N_2(g) and H_2(g). The labels of the bars refer to the most stable intermediates of the complex shown below the energy diagram.

In the energy diagram in Figure 9 all energies are given using atomic H as the reference state. In Figure 11 we show the hydrogenation path using molecular hydrogen as the reference state. For simplicity we have only included the case where there is no H on the S atoms on the cluster, but the general trends are not altered if the H atoms are included, cf. Figure 9. It can be seen that the most unstable complex on the path to ammonia synthesis is the I-NNH complex just as it is for the corresponding gas phase reaction.[37,38,56] The NNH complex is, however, stabilized significantly by the bonding to the Fe of model I.[37] This is an important catalytic effect of the complex − that it stabilizes the most unstable intermediate significantly.

The hydrogenation process studied by Siegbahn et al.[38] was for N_2 bound side on. The obtained energetics for hydrogenation was anyhow very similar to the one obtained by us. This indicates that the general energetics of hydrogenation does not depend on the details of the structure.

We note that for each of the intermediates we have found the structure with the lowest energy (see Figure 10), but in some cases the energy differences between different isomers are

(56) Pople, J. A.; Curtiss, L. A. *J. Chem. Phys.* **1991**, *95*, 4385−4388.

extremely small. This is the case for the two isomers $[IH_n]-NH-NH$ and $[IH_n]N-NH_2$ for $n = 0, 2$, where we find $[IH_n]-NH-NH$ to be the more stable for $n = 0$ but $[IH_n]N-NH_2$ to be the more stable for $n = 2$. The energy differences are too small to conclude that one is more stable than the other, and we also note that the interactions with the surrounding protein could change the relative stability of NNH_2 and NHNH adsorbed on the FeMoco.

8. Proton Transfer to Adsorbed N_2 and CO

It is clear from the discussion in the previous section that a proton donor close to the adsorbed N_2 is needed to feed in at least the first proton to the adsorbed N_2. As discussed above, such a donor might either be a protonated amino residue or an H_2O molecule. We have studied the proton transfer using the extremely simple model in Figure 12A using both H_3O^+ and NH_4^+ as proton donors.

Adsorbing N_2 or CO on the Fe atom closest to the H_3O^+ leads to a proton transfer from the H_3O^+ to the adsorbed N_2 or CO such that we end up with H_2O and adsorbed NNH or COH, respectively. Proton transfer is not observed if we substitute H_3O^+ with NH_4^+. If, on the other hand, we start with the proton attached to an adsorbed N_2 or CO, then the H atom transfers back to NH_3, but not to H_2O. Hence, the results may be summarized by

$$[XNN]^- + H_3O^+ \rightarrow XNNH + H_2O \quad (7)$$

$$[XCO]^- + H_3O^+ \rightarrow XCOH + H_2O \quad (8)$$

$$[XNN]^- + NH_4^+ \leftarrow XNNH + NH_3 \quad (9)$$

$$[XCO]^- + NH_4^+ \leftarrow XCOH + NH_3 \quad (10)$$

The calculations demonstrate that there is no barrier for proton transfer in the present setup. If there was a barrier the proton would stay on the site where it was added initially, regardless of whether the site was the acceptor or donor. We note that if we add an extra electron to the cluster (making it doubly negative) then proton transfer becomes spontaneous from NH_4^+ to adsorbed N_2 but not to adsorbed CO, showing that N_2 is more reactive than CO.

The energies for N_2 and CO adsorption and the critical step, the addition of the first H atom, are shown in Figure 12. It is seen that there are two effects. One is the stabilization of the adsorbed states discussed above. The other is that the least stable intermediate N−NH (and C−OH) is made much more stable when the proton comes from NH_4^+.

Figure 12 shows that under the conditions of the model calculation it is more facile to add a proton to N_2 than to CO. The barrier to form N−NH (B to C in Figure 12) is considerably smaller than the corresponding barrier to form C−OH, (B′ to C′ in Figure 12). This is in good qualitative agreement with the observation that N_2 can be hydrogenated in the enzyme while CO cannot.[3] If CO is present, it may be trapped in the adsorbed state after addition of only one proton (to the proton donor) and electron. Notice, however, that H_2 still may be formed on other Fe atoms (or S atoms).

The increased stability of the N−NH intermediate by the electron transfer to the FeMoco is the key to make the reaction go at low temperatures. In Figure 13 we compare the N_2 adsorption and the first electron and proton transfer step for two cases: where the proton donor is not included (red bars) and where it is included (green bars). It is clearly seen that the inclusion of a proton donor decreases the activation energy.

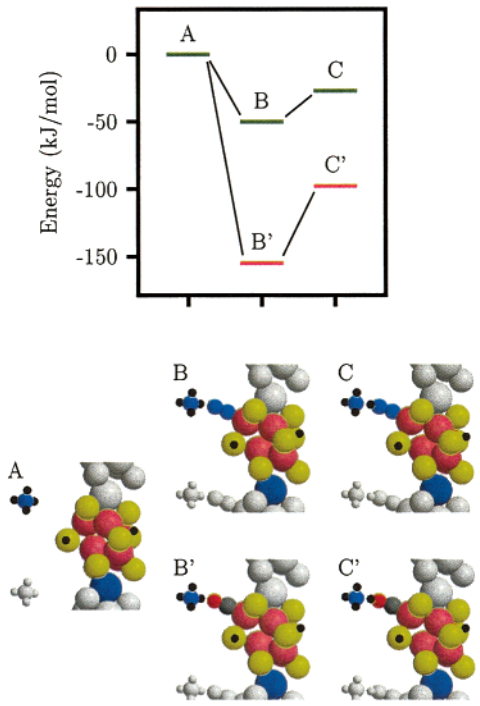

Figure 12. Energy diagram for protonation of N_2 (green bars) and CO (red bars). The reference levels are the energies of the structure in part A and the gas-phase molecules N_2 and CO. N_2 is adsorbed in part B and CO in part B′. The proton from the ammonium is transferred to the adsorbed N_2 in part C and to CO in part C′. The structures in parts C and C′ are calculated by constraining the N−H and the O−H distance, respectively, to the value obtained for the corresponding energy optimized structures without NH_4^+, otherwise the proton goes back to the ammonia.

There are two contributions to the lowering of the activation energy, an increase in the energy of the "H" $= e^- + H^+$ entering into the reaction, and the interaction (hydrogen bonding) between the NNH intermediate and the proton donor. The latter effect is illustrated by the decrease of the b level to the B level in Figure 13. The difference between the c and C levels is roughly due to the sum of the two effects.

The increase of the energy of the "H" $= e^- + H^+$ entering into the reaction can be illustrated in the following way. For process a−c (without the proton donor) the H atoms are taken from molecular H_2. In the process with the proton donor, the energy zero is a state with an electron on model I and the proton on the proton donor. The energy of this state is considerably higher than that for the H_2 molecule. This is illustrated in Figure 13 by including as the state A_0 the proton donor without the proton (an ammonia molecule) and the neutral FeMoco. The H atom missing relative to state A is again referred to as an H_2 molecule. The energy difference between A and A_0 is the extra energy, besides the H-bond, that the C level is stabilized with relative to c. This effect is not limited to the extremely simple cluster plus donor model studied here, but is easily generalized. We can say that the energy of the transition state (N−NH) is determined by the chemical potential of the electron and proton that is transferred. An important effect of the rest of the protein is therefore to give the electron (and proton) a high chemical potential to facilitate the process as much as possible.

It may be that the enzyme reaction is able to proceed at room temperature because the enzyme feeds hydrogens with a higher chemical potential than in H_2 into the reaction in the form of electrons with a high electrochemical potential and/or through the hydrolysis of ATP. This was recently substantiated by Spee

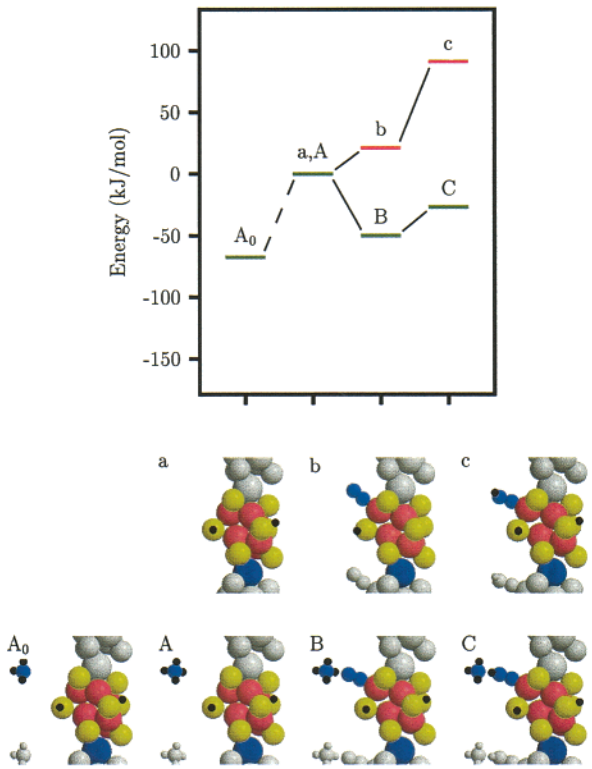

Figure 13. The energetics for hydrogenation/protonation of N_2 adsorbed on model I with a proton donor (green bars) and without a proton donor (red bars). Also included is the structure with a deprotonated proton donor (A_0). The energies of the structures without the proton donor (red bars) are relative to N_2(g), H_2(g), and model I (a). The energies of structures B and C are relative to the energy of structure A and N_2(*g*). The energy of structure A_0 is the energy needed for the reaction $A_0 + {}^1/_2H_2(g) \leftarrow A$.

et al.,[57] who measured the redox potential for all the clusters in the ADP·AlF_4 stabilized *Azotobacter vinelandii complex* resembling the transition state of the enzyme. They found that the redox potential of the Fe protein [4Fe-4S] cluster is significantly lowered in the complex compared to the free Fe protein [4Fe-4S] cluster, while the redox potentials of the P cluster and the FeMoco are hardly changed. Similar behavior has been measured for other complexes resembling the transition state.[58] This shows that the chemical potential of an electron located on the Fe protein 4Fe−4S cluster is lifted in the transition state. It should be noted that the Fe protein so far is the only known agent capable of transferring electrons to the MoFe protein.

9. Discussion and Summary

We have investigated in this paper a simple model of the FeMoco which is believed to be the catalytically active part of nitrogenase. We have been using two different clusters to mimic the central part of the FeMoco and have included the effect of the surroundings in a crude way by invoking a proton donor in the vicinity of the cofactor. Based on extensive density functional calculations of the interaction of these model clusters with a number of different substrates we can tentatively suggest a detailed atomistic explanation of a number of the observed properties of the FeMoco.

(57) Spee, J. H.; Arendsen, A. F.; Wassink, H.; Marritt, S. J.; Hagen, W. R.; Haaker, H. *FEBS Lett.* **1998**, *432*, 55−58.

(58) Chan, J. M.; Ryle, M. J.; Seefeldt, L. C. *J. Biol. Chem.* **1999**, *274*, 17593−17598. Lanzilotta, W. N.; Seefeldt, L. C. *Biochemistry* **1997**, *36*, 12976−12983.

The interaction of the FeMoco with CO is well-characterized experimentally, and we can account for a number of these observations:

(1) CO adsorbs strongly (Figure 5), in particular when an electron has been transferred to the FeMoco and a proton to the proton donor nearby (Figure 5b → Figure 5B), explaining why CO adsorption is only observed during turnover. CO adsorbs in the same site as N_2 but much stronger (Figure 12A → Figure 12B,B′). CO is therefore a poison for nitrogen fixation.

(2) The FeMoco can adsorb two CO (Figure 5C), but the second molecule binds weaker than the first (Figure 5B → Figure 5C), just as observed experimentally.

(3) The observed frequency shifts for both single and double occupation of the FeMoco by CO are in the range of the observations (Table 4, Figure 6).

(4) Proton transfer to the CO is considerably more difficult than that to N_2, explaining why CO hydrogenation is much more difficult (Figure 12).

(5) The strong H-bond to adsorbed CO (Figure 5B) hinders the otherwise exchangeable proton to interact directly with the FeMoco.

We have also studied the interaction of H_2 and D_2 with the FeMoco and can on this basis understand some of the observations concerning H_2 evolution and HD synthesis:

(1) H_2 (D_2) adsorption is facile (Figure 3g,j,l) and can take place at the same site as N_2 adsorption (Figure 2). H_2 is therefore competing with N_2 adsorption and is a poison for nitrogen fixation. The H_2 adsorption energy is weak compared to, e.g., CO adsorption (Figure 5b,B), and it is therefore only a weak poison.

(2) H_2 can be dissociated and the H atoms are most stable on the three equatorial μ_2S atoms (Figure 3).

(3) During turnover electrons and protons transferred to the FeMoco will result in H atoms, which again will be most stable on the three equatorial μ_2S atoms (Figure 3). If the electron and proton flow stops, H_2 will evolve, if two or more H atoms are on the cluster in agreement with the Thorneley−Lowe scheme.[3,21]

(4) HD production during turnover in a D_2 atmosphere[3,19,21] can be the result of D_2 dissociation (for instance Figure 3g→f→d) followed by HD (or D_2) formation. H_2 formation will be improbable since the D atoms will be closest to the adsorption/desorption site after D_2 dissociation. Dissociation is only possible if there is an empty site on at least one of the μ_2S atoms. During turnover that is not very likely. But if N_2 is present, ammonia synthesis (Figure 10) will result in free sites due to migration of H from the μ_2S atoms to N_2 (Figure 10f→i). This may explain why the presence of N_2 can increase the HD synthesis rate.

(5) H_2 formation is competing with ammonia synthesis during turnover in an N_2 atmosphere in agreement with experiment.[3,19,21] There is nothing in our findings pointing to a stoichiometric minimum H_2 production as assumed in the Thorneley−Lowe scheme.[3,21]

When it comes to the N_2 adsorption and the ammonia synthesis, we are led to the following picture of the process:

(1) N_2 can adsorb in an end-on fashion. Dissociation is very unlikely due to the fact that atomic nitrogen interacts very repulsively with the FeMoco (Figure 7h).

(2) N_2 binds strongest during turnover: an electron needs to be transferred to the FeMoco and a proton to the vicinity in order for N_2 to spend an appreciable time in the adsorbed state (Figure 8).

(3) The formation of adsorbed NNH is the rate-limiting step in the ammonia synthesis provided electrons and protons are readily available (Figure 11c). The transfer of a single electron and proton to adsorbed N_2 will result in the formation of NNH, but if there are no extra H atoms on the FeMoco this state will quickly decay leading to an H atom on one of the μ_2S atoms and a desorbing N_2 molecule. If there are three H atoms on the cluster, on the other hand, the system can transfer into adsorbed hydrazine immediately (Figure 10f→i), and this state is so stable that the process is irreversible. The fact that only the fourth electron/proton transfer will make the reaction go irreversibly is in excellent agreement with the Thorneley−Lowe kinetics[3,21] and therefore with the rate measurements behind this kinetics.

(4) The ratio of NH_3 to H_2 formation will depend on the very detailed energetics of the process. The question is whether a hydride (Figure 3; the least stable intermediate in H_2 production) or adsorbed NNH (Figure 11; the least stable intermediate in NH_3 production) is the most stable. This may well depend critically on the surroundings of the FeMoco and therefore on the kind of nitrogenase studied. It must also depend on the electron flux. As discussed above, ammonia synthesis requires several H atoms on the μ_2S atoms before N_2 is irreversibly activated by an electron and proton transfer followed by migration of H to the N_2. If the electron (and proton) flux is low, the probability of having two or more H atoms on the FeMoco before H_2 is desorbed is low and the NH_3 to H_2 ratio will be low as observed experimentally.[19,21]

(5) The proton transfer to the adsorbed N_2 (and presumably even to the FeMoco without N_2) is nonactivated.

Recently, Newton et al.[51] reported that if histidine-195 of *Azotobacter vinelandii* nitrogenase is replaced with glutamine then the FeMoco is capable of binding N_2, but the ability to reduce N_2 is significantly reduced. If the histidine is replaced with other amino residues, among those asparagine, the FeMoco also loses the ability to bind N_2. Our results based on the simple model of the proton donor demonstrate that a proton donor in the vicinity is capable of forming an H-bond to adsorbed N_2. The side chain of histidine is the only amino acid side chain capable of both accepting and donating protons at a neutral pH,[59] but both glutamine and asparagine have a terminal neutral amide group able to form H-bonds. Asparagine and glutamine are completely equal, except that the side chain of asparagine is one CH_2 term shorter than glutamine. We therefore suggest that the observations made by Newton et al. may be explained by the following points: (1) Histidine is able to H-bond and donate protons to adsorbed N_2. (2) Glutamine is able to H-bond to adsorbed N_2, but unable to donate protons. (3) Asparagine is too short to form an H-bond to the adsorbed N_2, and N_2 is therefore not adsorbed on the FeMoco.

We are now also in a position to comment on why such a large and complex transition metal sulfur cluster is needed for N_2 activation in the enzyme. Our calculations point to two reasons. First, it is clear that the cluster and the surroundings must be loaded with electrons and protons (H on the μ_2S's and an electron on the FeMoco and a proton on the donor) before N_2 can be adsorbed and hydrogenated irreversibly. The cluster therefore has to be large to accommodate the H's. The second reason is more subtle. N_2 is a very inert molecule. For N_2 to be able to interact attractively with a cluster, it must contain at least one transition metal atom that is unsaturated. That, on the other hand, will make the cluster very reactive in general. The FeMoco has solved this problem elegantly. The Fe atoms are not saturated, but are inaccessible to the surroundings because the Fe(Mo) core is covered by an S shell. The S atoms prevent other parts of the enzyme, water, and other adsorbates from interacting directly with the unsaturated Fe core. In fact, the Fe−Fe distances in the core are like those in the metal and not like those in a sulfide, so the cluster can be viewed as a passivated "metallic" Fe cluster. The passivation by S is not due to a complete saturation of the Fe atoms ability to bond, but due to a simple "geometrical" blocking of the Fe core. For a molecule like N_2 (or CO or H_2) to interact with the unsaturated Fe core, the whole cluster must distort (see, e.g., Figure 2). During the distortion one of the Fe atoms sticks out and interacts with the adsorbing molecule. Such a distortion is only possible for a relatively large (and flexible) cluster.

It is clear that our model is extremely simple. This together with the limited accuracy of the density functional calculations means that the results should only be taken as qualitative, and serve as a help in establishing a detailed picture of the process.

To make the results more quantitative it will be important to develop a better model of the surroundings of the FeMoco where solvent effects and the dielectric response of the rest of the protein are included in more detail. It is also clear that questions relating to the electron and proton transfer to the vicinity of the FeMoco and the role of ATP and the reduction potential of the electron source are extremely important for a more complete picture of the whole process. It would also be extremely interesting to model the effect of substituting Mo for V or Fe or to start to change the ligands in some detail.

Acknowledgment. Many stimulating discussions with B. Hammer, A. Logadottir, and K. W. Jacobsen are gratefully acknowledged. The present work was financed in part by The Danish Research Councils through Grant No. 9501775. The Center for Atomic-scale Materials Physics (CAMP) is sponsored by the Danish National Research Center.

JA001163Q

(59) Palmer, T. *Enzymes*, 4th ed.; Prentice Hall/Ellis Horwood: London, 1995.

(60) Berman, H. M.; Westbrook, J.; Eng, Z. F.; Gilliland, G.; Bhat, T. N.; Weissig, H.; Shindyalov, I. N.; Bourne, P. E. *Nucl. Acids Res.* **2000**, *28*, 235−242.

(61) Bernstein, F. C.; Koetzle, T. F.; Williams, G. J.; Meyer, E. E., Jr.; Brice, M. D.; Rodgers, J. R.; Kennard, O.; Shimanouchi, T.; Tasumi, M. *J. Mol. Biol.* **1977**, *112*, 535.

(62) URL: http://www.rcsb.org/pdb/.

(63) PDB ID: 1QGU. Published in ref 8. General PDB refs 60−62.